Article

pubs.acs.org/Biomac

Bionanocomposites: Differential Effects of Cellulose Nanocrystals on Protein Diblock Copolymers

Jennifer S. Haghpanah,[†] Raymond Tu,[‡] Sandra Da Silva,[*] Deng Yan,[§] Silvana Mueller,[∥] Christoph Weder,[∥] E. Johan Foster,[∥] Iulia Sacui,[⊥] Jeffery W. Gilman,[⊥] and Jin Kim Montclare*[,†,#]

[†]Department of Chemical and Biomolecular Engineering, Polytechnic Institute of New York University, Brooklyn, New York 11201, United States

[‡]Department of Chemical Engineering, City College of New York, New York, New York 10031, United States

[*]Biomaterials and Biosystems Division, National Institute of Standards and Technology, Gaithersburg, Maryland 20899, United States

[§]Skirball Institute of Biomolecular Medicine, Microscopy Core Facilities, NYU Medical Center, New York, New York, 10016, United States

[∥]Adolphe Merkle Institute, University of Fribourg, CH-1723 Marly, Switzerland

[⊥]Materials Science and Engineering Division, National Institute of Standards and Technology, Gaithersburg, Maryland 20899, United States

[#]Department of Biochemistry, SUNY Downstate Medical Center, Brooklyn, New York 11203, United States

Supporting Information

ABSTRACT: We investigate the effects of mixing a colloidal suspension of tunicate-derived cellulose nanocrystals (t-CNCs) with aqueous colloidal suspensions of two protein diblock copolymers, EC and CE, which bear two different self-assembling domains (SADs) derived from elastin (E) and the coiled-coil region of cartilage oligomeric matrix protein (C). The resulting aqueous mixtures reveal improved mechanical integrity for the CE+t-CNC mixture, which exhibits an elastic gel network. This is in contrast to EC+t-CNC, which does not form a gel, indicating that block orientation influences the ability to interact with t-CNCs. Surface analysis and interfacial characterization indicate that the differential mechanical properties of the two samples are due to the prevalent display of the E domain by CE, which interacts more with t-CNCs leading to a stronger network with t-CNCs. On the other hand, EC, which is predominantly C-rich on its surface, does not interact as much with t-CNCs. This suggests that the surface characteristics of the protein polymers, due to folding and self-assembly, are important factors for the interactions with t-CNCs, and a significant influence on the overall mechanical properties. These results have interesting implications for the understanding of cellulose hydrophobic interactions, natural biomaterials and the development of artificially assembled bionanocomposites.

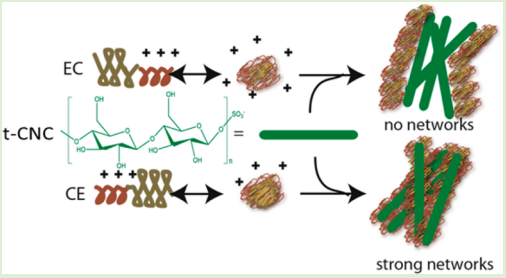

INTRODUCTION

Nature has developed an array of structural materials with a remarkable range of chemical and physical properties.[1−4] Protein materials both in nature and man-made can assemble into various supramolecular structures that can modulate coloration enabling dynamic camouflage,[5−7] or exhibit extreme strength and load-bearing properties.[8−10] While proteins play a major role in the properties of the biomaterial, they are often intermingled with other biopolymers such as lipids, polysaccharides, and nucleic acids as well as inorganic materials.[11−16] Thus, the overall physicochemical properties are the result of a mixture or composite of biopolymers.

Recently, we developed two protein block copolymers—EC and CE—comprised of two distinct self-assembling domains (SADs) derived from elastin (E) and the coiled-coil domain of cartilage oligomeric matrix protein (C) (Figure 1). While the diblocks were compositionally nearly identical, they exhibited *different* secondary structures and supramolecular assemblies.[17,18] This difference was also observed in their bulk aqueous mechanical properties; EC formed an elastic network, while CE was a viscous fluid.[18] This behavior may be due to the fact that EC self-assembled into larger particles, while CE formed smaller particles.[18] Previously, we have shown that the specific orientation of the blocks significantly affected the overall secondary structure, self-assembly, and materials properties.[17−20] Since these two protein block polymers exhibited dissimilar properties on the nano- to macro-scale, we sought to explore whether these two proteins differentially interact with other well-defined biopolymers and bionanocomposites with dissimilar properties.

Received: August 31, 2013
Revised: October 11, 2013
Published: October 18, 2013

dx.doi.org/10.1021/bm401304w | *Biomacromolecules* 2013, 14, 4360−4367

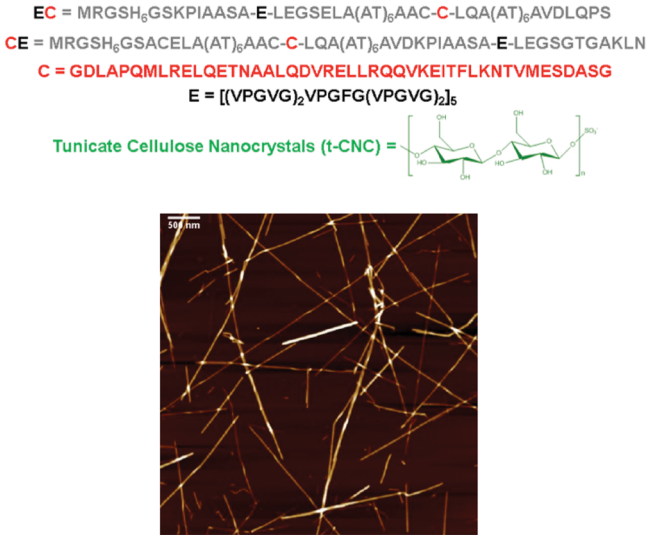

Figure 1. Protein constructs EC and CE illustrating sequences and chemical structure (top); Atomic force microscopy image of tunicate cellulose nanocrystals (t-CNC) on silicon/polylysine surface (bottom).

We selected cellulose as it is a polysaccharide that is abundant, renewable, and in the form of naturally occurring nanocrystals, which exhibit high mechanical stability and stiffness.[21] In particular, cellulose nanocrystals isolated from tunicate (t-CNC) possess a high aspect ratios,[22] ~83, an on-axis Young's modulus of 80 to 150 GPa, and consequently are well suited as reinforcement in composites.[23−27] As members of type I β-cellulose allomorphs, they are 95% crystalline with surface exposed hydroxyl groups that can strongly interact with polar sites of polymer chains via hydrogen bonding.[23,28] Due to their unique physical features and chemical properties, t-CNC has been used as a filler to enhance the mechanical properties of a wide range of materials.[26,29−31] For example, t-CNC has been employed to reinforce and enhance the mechanical properties of a range of polymers, including polystyrene, poly(butyl acrylate) and poly(acrylic acid).[24] Nanocomposites recently made with starch and sorbitol plasticizer have also been modified with t-CNC for reinforcement.[26] The materials exhibit an increase in crystallinity and alteration of the glass transition temperature (T_g) upon t-CNC addition.

Certain natural proteins and cellulose interact via defined regions known as cellulose binding domains (CBDs).[32] Over one hundred different CBDs have been identified and classified into eight categories based on sequence homology with sequences ranging from 33 to over 170 amino acid residues.[33−35] Natural CBDs provide evidence for protein·cellulose complexation, which appears to be predominantly mediated through hydrophobic interactions, leading to changes in the overall physicochemical property of the complex.

As t-CNCs have been shown to improve bulk properties of other nonbiopolymers[23−26,36] and interact with proteins via CBDs,[32] we investigate the impact of t-CNCs on the EC and CE protein diblock copolymers and assess their overall physicochemical properties. As the interactions of the t-CNCs with EC and CE take time upon mixing, we investigate their properties as a function of time. Here, we describe the fabrication and characterization of aqueous mixtures of EC+t-CNC and CE+t-CNC (Figure 1). We discover that EC and CE possess different modes of assembly in the presence of t-CNC, leading to differences in their mechanical properties. This differential behavior is due to the supramolecular assembly and surface character of the diblock copolymers. Specifically, CE exhibits more E-like character on its surface than EC, which has more C-like character on its surface. This enables CE to more strongly interact with t-CNC, leading to gel behavior.

MATERIALS AND METHODS

Materials. Methanol (99.9% pure), sucrose, Trizma base, ampicillin, chloramphenicol, isopropyl β-D-1-thiogalactopyranoside, thiamine, calcium chloride, magnesium sulfate, imidazole, urea, sodium phosphate, ammonium chloride, sodium chloride, potassium phosphate monobasic, brilliant blue, ammonium persulfate and 17.4 N glacial acetic acid were purchased from Fisher. HiTrap IMAC FF 5 mL columns were obtained from GE life sciences. Ni-NTA beads, fluorescein isothiocyanate, dibutyltindilaurate and DMF (99.8% pure) were purchased from Sigma Aldrich. Precision plus protein standards and 30% (mass fraction) bis-acrylamide were from Bio-Rad life science. Snake Skin pleated dialysis tubing with 3KDa MWCO, micro BCA and bovine serum albumin were obtained from Thermo Scientific. Amicon centrifugal and 0.2 μm polyethersulfone filters were purchased from Millipore. Fluorescent polystyrene beads (1.0 μm diameter) were from Invitrogen.

Preparation of Protein Polymers. Expression and purification methods were carried out as described previously.[17,18] While C, EC, and CE were expressed in M9 supplemented media and purified via HiTrap IMAC FF Co^{2+} column, E was expressed in LB and purified over a column with Ni-NTA agarose beads. All proteins were purified under denaturing conditions at 4 °C to prevent aggregation of the protein on the column as before.[17,18] All proteins were analyzed on a 12% (mass fraction) SDS polyacrylamide gel and analyzed by Image Quant to confirm 95% purity (Supporting Information, Figure S1). Purified proteins C, EC, and CE were dialyzed into water and lyophilized down to dryness, while E was stepwise dialyzed into water with concentrations of urea ranging from 3 mol/L to 0 mol/L and lyophilized down to dryness. Purified proteins were resuspended in Milli-Q distilled (RNase/DNase free) water and were analyzed by micro-BCA with known concentrations of BSA standards to determine concentrations.

Approximately 2 mg mL^{-1} of EC and CE were labeled with 1 mg mL^{-1} Alexa fluor 555 carboxylic acid succinimidyl ester then resuspended in 10 mmol/L phosphate buffer with 0.1 mol/L sodium bicarbonate and incubated overnight at 4 °C in the dark for confocal experiments. The reaction mixture was then subjected to purification on a Sephadex column. Elutions containing both the highest absorbance for protein at 254 nm and the highest absorbance for dye at 555 nm were used for further studies. Purity and concentration was determined via SDS-PAGE using ImageQuant (Supporting Information, Figures S2, S3).

Isolation of Tunicate Cellulose (t-CNC). Unmodified cellulose nanocrystals from tunicates (t-CNC) were prepared as previously described (Figure 1).[27,37] Due to their isolation by hydrolysis with sulfuric acid, the t-CNC samples possess a surface density of approximately 85 mmol kg^{-1} SO_4^- and the typical dimensions of the nanocrystals were 20 nm x 2.2 μm.[51] Typical functionalization of the t-CNCs was carried out using 0.1 eq (mol basis) fluorescein isothiocyanate (Aldrich) per glucose unit in cellulose, charged into a flask with 120 mL of DMF and 0.5 g of t-CNCs. To this dibutyltindilaurate (1 drop)

dx.doi.org/10.1021/bm401304w | Biomacromolecules 2013, 14, 4360−4367

was added, and the mixture was heated to 100 °C and stirred at this temperature overnight under N_2 atmosphere. The reaction mixture was then allowed to cool and DMF and unreacted FITC were removed by centrifugation and subsequently dialyzed against distilled water for 7 d (exchanging distilled water every 12 h). Surface functionalization was quantified by UV spectroscopy of an aqueous dispersion of the fluorescein-modified t-CNC, and compared to a calibration curve prepared using a series of solutions of dilute concentrations of fluorescein in solvent (See Supporting Figure S2c to give a functionalization of 12.36 mmol/kg. The labeled t-CNCs were lyophilized and resuspended in distilled (RNase/DNase free) water to final concentrations of 0.2 mg mL^{-1}, 0.1 mg mL^{-1} and 0.02 mg mL^{-1}. Labelled t-CNC were only used for confocal imaging experiments.

Microrheology. All solutions for passive microrheology included 12 μL of sample with 0.33% (mass fraction %) of fluorescent amidated polystyrene beads. Final concentration ratio of protein polymer:t-CNC of 0.8 mg mL^{-1}: 0.2 mg mL^{-1} in distilled (RNase/DNase free) water was generated at room temperature. Particle trajectories were monitored over a time period of 100 min at room temperature. Epifluorescence on an inverted Leica DM- IRB microscope was used with 2 objective lenses, 64 x and 40 x. Multiple movies were recorded with a QiCam (640 × 480 pixels at 30 fps). For these experiments, the trajectories of the beads for each sample were obtained across two different trials with two different expression/purification sample preps. Each trial entailed four videos acquired in different locations of the slide per time point every 20 min between 10 and 100 min, except for individual components, which had videos taken at 10 and 100 min. For our experiments, passive microrheology was employed[38,39] and particle trajectories were obtained with IDL (Interactive Data Language) image software analysis.[40] Mean square displacement plots were generated and used to determine the storage and loss moduli as a function of composition and time.[41−46] The plots were employed to avoid artifacts in the data and view the dynamic change in mechanical properties over time. The mean square displacement plots were fitted in Microsoft excel via power trend line ($y = mx^b$) and logarithmic slopes (b) were acquired.[47,48]

Time−cure superposition was used to determine the switch from liquid to soft-gel and the critical relaxation exponent (n) of CE+t-CNC.[49−52] This was determined by taking the mean square displacement plots and multiplying the values by horizontal (a^{-1}) and vertical (b^{-1}) shift factors to produce two master curves denoted as "pre-gel" and "post-gel."[39,47−50] Time-cure superposition analysis was employed to ameliorate curing during experimental measurement, taking images of the sample at discrete times through the experiment.[50] The convergence of the master curves "pre-gel" and "post-gel," led to the critical relaxation exponent (n).[46,49,53]

Confocal Microscopy. Samples were dissolved in the appropriate volumes to obtain a final concentration of 0.8 mg/mL Alexa-fluor 555-protein and 0.2 mg/mL fluorescein-t-CNC in distilled (RNase/DNase free) water (Supporting Information, Figure S4). Protein samples were transferred onto a microscopy slide with a coverslip and imaged with a Leica TCS SP5 II confocal microscope as well as on a Zeiss LSM 710 NLO microscope. Fluorescein-t-CNC exhibited emission from 495 to 555 nm (excitation at 488 nm). Alexa-fluor 555-protein had emission from 568 to 625 nm (excitation at 561 nm).

Circular Dichroism (CD). While 0.08 mg mL^{-1} of each protein polymer was investigated in the absence and presence of the t-CNC, the final concentration ratios of polymer + t-CNC employed was 0.08 mg mL^{-1} + 0.02 mg mL^{-1} in distilled (RNase/DNase free) water. Wavelength scans for E, C, EC and CE were performed from 190 to 250 nm acquired at 4 °C. Since the samples underwent phase separation at temperatures above 4 °C, further quantitative analysis was not performed for CD at 25 °C. Two trials of data were collected on a J-815 CD Spectrometer, bearing a PTC-423S single position Peltier temperature control system. Samples were loaded into a Helma quartz cuvette with 1 mm path length. Raw data of proteins alone was subtracted from the water background and raw data of protein polymer + t-CNC was subtracted from t-CNC wavelength scan (Supporting Information, Figure S7) and passed through a Savitsky−Golay smoothing filter with a smoothing width of 11.[17,54]

Zeta Potential. Two trials of 2 to 3 scans with 10 runs per scan were performed for each protein polymer sample in the absence and presence of t-CNC. Samples were prepared with the same ratios as microrheology (0.4 mg mL^{-1} protein polymer to 0.1 mg mL^{-1} t-CNC) in distilled (RNase/DNase free) water. The pH of water was adjusted to 6.1, 10 min prior to the experiments. The samples were sonicated at 25 °C for 10 min before each run to make sure that all samples were well-dispersed in solution. All samples were loaded into 1.5 mL polystyrene, four-sided clear cuvettes with 10 mm path length (BI-SCP) and read on a Zeta Plus instrument (Brookhaven Instruments Cooperation). Three trials of viscosities for proteins in the absence and presence of t-CNC were performed from three different sample preps. Average viscosities were determined from microrheology rrm files using the following equation: Viscosity = $DK_BT/\pi 3a$MSD, where D is the dimensions, K_B is Boltzmann's constant, T is the absolute temperature in Kelvin, a is the radius of the sphere, and the MSD is the mean square displacement as determined from the slope of the plot of the sum of the trajectories in the x and y direction squared as a function of time.[42] Viscosities were taken for all the mixtures and individual components in their viscous regime to determine the zeta potential of the aggregate in the heterogeneous solution. The equation used to calculate the zeta potential was determined using the Smoluchowski limit equation: $\zeta = \mu^*\eta/\varepsilon$, where ζ is zeta potential, μ is the electrophoretic mobility of the liquid, η is the average viscosity calculated and ε is the permittivity of water at 25 °C.

RESULTS

Impact on Mechanical Strength. To evaluate the dynamic change of the viscoelastic properties of EC and CE aqueous mixtures as a function of time, we performed kinetic microrheology experiments with EC, and CE in the absence and presence of unlabeled t-CNCs. The concentrations of the protein and t-CNCs used for microrheology were chosen to be all within the viscous regime (Supporting Information, Figure S8) such that alterations of the mechanical properties could be attributed to the interactions between the protein and the t-CNCs. As a control, aqueous solutions of the C and E homopolymers in the presence of t-CNC were also assessed. The C+t-CNC mixture was a viscous solution with no evidence of network formation (Figure 2), while E+t-CNC was viscoelastic at 100 min (Figure 2). The EC+t-CNC mixture exhibited viscous character at all time frames, similar to the C +t-CNC mixture (Figure 2). By contrast, CE+t-CNC

dx.doi.org/10.1021/bm401304w | Biomacromolecules 2013, 14, 4360−4367

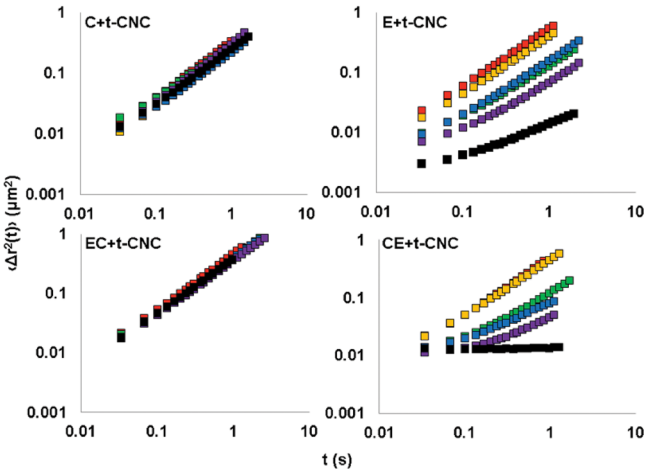

Figure 2. Plots of the mean square displacement as a function of time representing (red,10 min), (yellow, 20 min), (green, 40 min), (blue, 60 min), (purple, 80 min) and (black, 100 min) at room temperature for C+t-CNC, E+t-CNC, EC+t-CNC and CE+t-CNC.

demonstrated the formation of elastic network at 100 min, indicating that the t-CNCs indeed interact with the CE protein polymer leading to fundamental change of the mechanical properties (Figure 2). Thus, orientation of the SADs within the protein block polymer affected the interactions, structures and mechanical properties in which CE forms stronger networks in the presence of t-CNC over EC. Notably, CE+t-CNC was more mechanically stable than that of the homopolymer E+t-CNC mixture, indicating that the presence of the C domain in the diblock copolymer was critical for the assembly and interaction with t-CNC.

To gain insight into the mode by which the protein polymers and t-CNC interact, plots of the logarithmic slope (b) values from the mean square displacement data as a function of the various time frames were analyzed (Figure 3). The logarithmic slopes were determined by fitting each of the mean square displacement plots to a power function and acquiring an equation for the line. The change in the logarithmic slope as a function of time indicated that there was an interaction between the protein polymer and the t-CNC. The critical relaxation exponent (n) was determined using time-cure superposition analysis.[39,49,50] Time-cure superposition is a tool that has been applied to one/two particle microrheology, where moduli curves are constructed from cure data via multiplying the MSD plots by horizontal and vertical shift factors.[53,63] The critical relaxation exponent can be determined when n = b, the sample reached rheological percolation.[46−48,53] The values for the critical relaxation exponent can range from 0.1 to 1.0, which is contingent on the components in the system.[55,56] While C+t-CNC and EC+t-CNC did not exhibit network formation, E+t-CNC began to approach rheological percolation, but failed to form complete networks, leading to viscoelastic character (Figure 3). CE+t-CNC revealed rheological percolation after curing (hardening or toughening) of gel, resulting in a critical relaxation exponent (n) of 0.24 (Supporting Information, Figure S9). A switch from liquid to soft-gel was observed between 50 and 60 min and a more abrupt transition to an elastic network was observed at 80 min (Supporting Information, Figure S7). A low n value is typical for long-chain dense stiff networks and has been previously observed for ethyl(hydroxyethy1)cellulose (EHEC)/sodium dodecyl sulfate (SDS) (n = 0.24 to 0.41),[57] micronetworks of end-linking polystyrene (n = 0.2 to 0.5),[58] crystallization of a bacterial polyester (n = 0.11),[59] and crystallization induced polypropylene (n = 0.125).[60] In addition, this system contains some of the requirements identified by Raghavan or gelation by entanglements (or "topological interactions"),[61] i.e., the t-CNCs have high aspect ratios and are stiff, and the CE and EC form persistent particles, as evidenced by DLS and TEM results from our previous studies.[17,18]

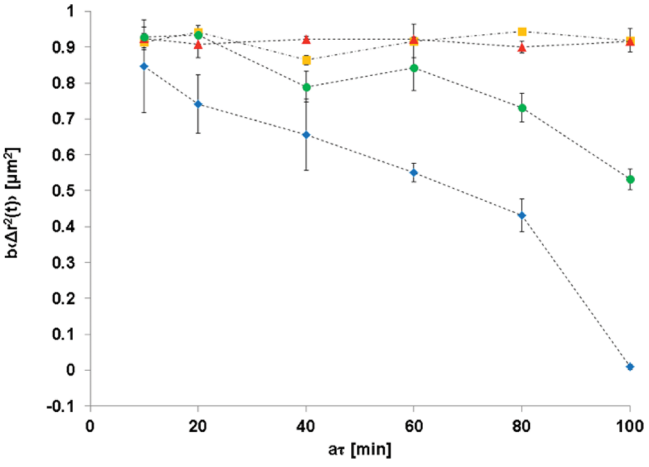

Figure 3. Plots of logarithmic slope b from mean square displacement data of proteins in the presence of t-CNC as a function time at room temperature. Points represent (■ C+t-CNC, ● E+t-CNC, ▲ EC+t-CNC, and ◆ CE+t-CNC). Error bars denote standard deviations for two different sample preps with four different videos acquired at different locations.

Morphological Analysis of Protein Polymers and t-CNC Mixtures. To further assess the morphology of the protein polymers EC and CE with t-CNC mixtures, both diblocks were labeled with Alexafluor 555, while the t-CNCs were labeled with fluorescein, and the mixtures were evaluated under a confocal microscope (Figure 4). Confocal images of fluorescently labeled EC+t-CNC and CE+t-CNC revealed the microscale morphology of the samples. Qualitatively, the CE was more interspersed than the EC with the t-CNCs, in which larger domains of t-CNC were observed in the EC+t-CNC. This suggested that CE intermingled with the t-CNC better than that of EC+t-CNC.

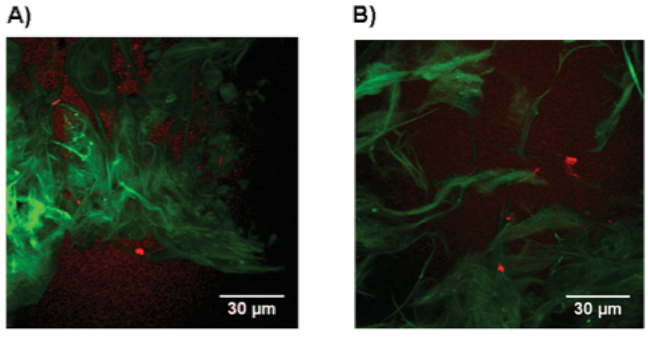

Figure 4. Confocal images of (A) EC+t-CNC and (B) CE+t-CNC. In the image, EC and CE are labeled with 555 Alexa Fluor carboxylic acid, succinimidyl ester (red), and t-CNC is labeled with fluorescein (green).

dx.doi.org/10.1021/bm401304w | Biomacromolecules 2013, 14, 4360−4367

Effects of t-CNC on Secondary Structure. To understand how each component of the block polymers interacts with the t-CNCs, the secondary structure of the proteins in the absence and presence of t-CNCs were evaluated. Circular dichroism (CD) was employed, as it allows the measurement of structural ($n\rightarrow\pi^* + \pi\rightarrow\pi^*$) transitions in the protein that may occur due to the interaction with t-CNCs.[62] As the t-CNCs alone did not exhibit a significant signature in the far-UV range of 190 to 250 nm (Supporting Information, Figure S7), it was possible to monitor the alterations in the protein polymers caused by the presence of t-CNCs. These experiments were performed in water to be consistent with the conditions that were used for microrheology. As a control, wavelength scans of C and E were assessed in the absence and presence of t-CNCs. The C homopolymer illustrated a double minima with a signal of (-8.48 ± 0.95) mdeg and (-14.67 ± 0.14) mdeg at 208 and 222 nm, respectively (Figure 5). Unlike previous data,[17,63,64] which showed minima of equal magnitude, the minimum was more negative at 222 nm, indicative of protein aggregation,[64] due to the measurements being performed in the absence of buffer. Upon addition of t-CNCs, the wavelength scans did not alter significantly (Figure 5, Table 1). In contrast, the E homopolymer possessed a single minimum with a signal of (1.28 ± 0.14) mdeg at 225 nm, consistent with previous data.[17] Addition of t-CNCs led to an increase in the minimum and slight blue shift with a signal of (2.18 ± 0.33) mdeg at 223 nm (Figure 5, Table 1), suggesting an interaction between the two biopolymers. Wavelength scans of EC and CE revealed a double minima for both constructs (Figure 5, Table 1).[17] In the presence of t-CNCs, an increase in signal was observed for both EC and CE protein polymers. While the EC+t-CNC demonstrated a 1.27 mdeg increase in signal at 222 nm, CE +t-CNC showed a significantly larger increase in signal of 8.83 mdeg at 222 nm (Figure 5, Table 1). The t-CNC appeared to interact substantially more with CE when compared to EC, confirming the orientation dependence of the protein diblocks when exposed to t-CNCs.

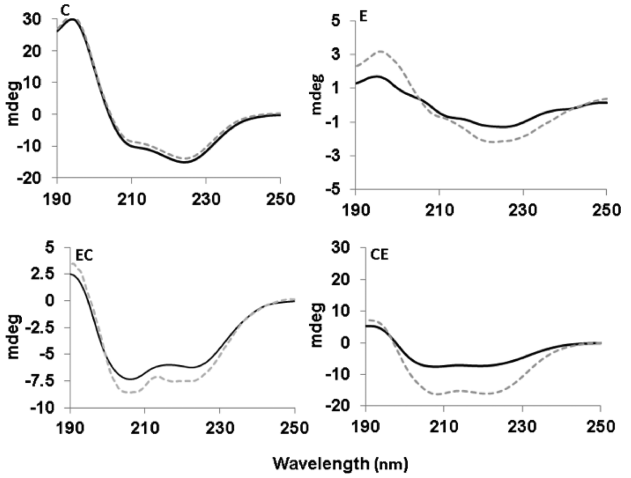

Figure 5. Circular dichroism (CD) wavelength spectra of proteins in the absence (black solid) and presence (gray dashed) of t-CNC at 4 °C. The data represents an average of two trials.

Self-Assembly and Surface Charge. The zeta potential of the protein polymers in the absence and presence of t-CNCs were investigated to gain insight into the surface charge of each biopolymer component and the bionanocomposite mixtures. As the t-CNCs possess a surface charge of 85 mmol SO_4^- kg^{-1},[65] they have a highly stable negative zeta potential of −83.30 mV (Figure 6). As expected, the C homopolymer possessed a positive zeta potential of +77.32 mV, while the E homopolymer exhibited a slight negative zeta potential of −3.84 mV. While both diblocks possessed an overall positive charge, EC and CE revealed zeta potentials of +37.66 mV and +9.84 mV, respectively, affirming that block orientation impacts the self-assembly (Figure 6).[18] Based on the surface charge, EC appeared to possess more C-like character in comparison to CE.

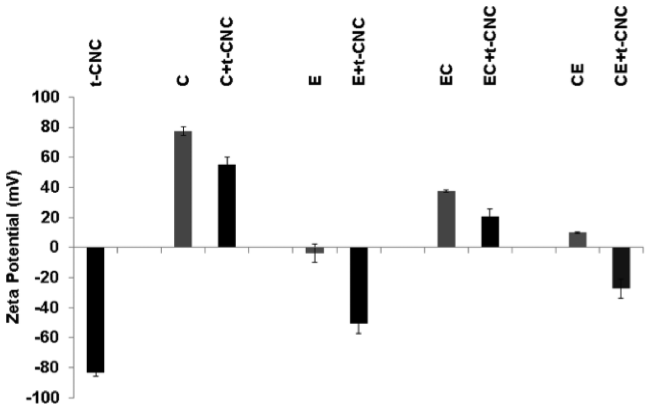

Figure 6. Zeta potential of t-CNC, C, C+t-CNC, E, E+t-CNC, EC, EC +t-CNC, CE, and CE+ t-CNC at RT. Data average and standard error represent two trials from 2 to 3 scans.

Table 1. Circular Dichroism (CD) Data of Proteins in the Absence and Presence t-CNC in mdeg at 4 °C, Values at 208 and 222 nm[a]

sample	$\lambda_{min.1}$ (nm)	$\lambda_{min.2}$ (nm)	$[\theta]_{222}$ mdeg	standard deviation	$[\theta]_{208}$ mdeg	standard deviation	$[\theta]_{222}/[\theta]_{208}$
t-CNC	208	222	1.05	0.23	1.24	0.044	0.85
C	208	222	−14.67	0.14	−8.48	0.95	1.73
C+t-CNC	208	222	−13.38	0.19	−6.42	0.64	2.08
E	--------	225	−1.28	0.14	--------	--------	--------
E+t-CNC	---------	223	−2.18	0.33	--------	--------	--------
EC	208	222	−6.23	0.03	−7.18	0.03	0.87
EC+t-CNC	208	222	−7.50	0.92	−8.51	1.43	0.88
CE	208	222	−7.13	0.38	−7.55	0.01	0.94
CE+t-CNC	208	222	−15.96	1.08	−16.22	0.75	0.98

[a]Data represents the average of two independent experiments.

dx.doi.org/10.1021/bm401304w | Biomacromolecules 2013, 14, 4360−4367

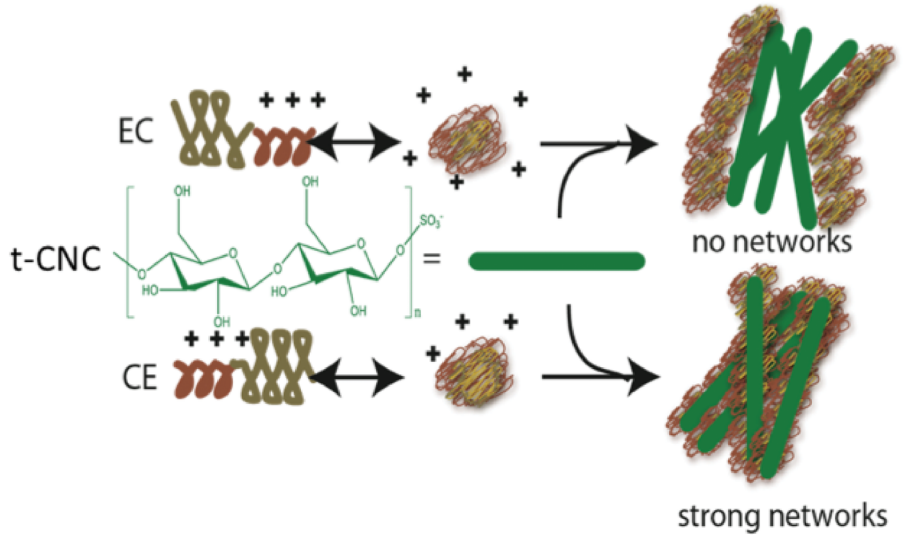

Figure 7. Cartoon depicting the interactions of EC and CE with t-CNC.

After mixing the proteins with t-CNCs, the surface charge of the complexes was assessed. The C+t-CNC revealed a zeta potential of +54.88 mV; exhibiting a loss in charge and stability when compared to the C homopolymer alone (Figure 6). By contrast, E+t-CNC exhibited an increase in stability with a more negative zeta potential of −50.78 mV relative to the E homopolymer. In the case of the protein diblocks, EC+t-CNC displayed a loss in stability with a zeta potential of +20.37 mV, while CE+t-CNC showed an increase in stability and zeta potential of −27.38 mV relative to their protein counterparts in the absence of t-CNC (Figure 6). The E and CE in the presence of t-CNCs led to stabilization relative to their protein parents indicative of interaction with t-CNC. Based on these results in conjunction with the protein polymer data alone, the less positive CE protein particles exhibited E-like character on the surface facilitating interaction with t-CNCs.

DISCUSSION

We discovered that EC and CE possess different kinetics in the rates of assembly in the presence of t-CNC, leading to differences in the mechanical properties of the EC+t-CNC and CE+t-CNC aqueous mixtures. While EC+t-CNC exhibits viscous behavior, CE+t-CNC reveals formation of an elastic network, indicating that block orientation influences the ability to interact with t-CNC. The subtle differences in supramolecular assembly and surface character of each diblock copolymer are crucial to complexation with t-CNCs and overall bulk properties.

Nature of Protein Polymer and t-CNC Interaction. The notable difference in viscoelastic properties of EC and CE in the presence of t-CNCs can be attributed to the insights gleaned from how each domain is affected on a molecular level in terms of structure and overall self-assembly. Our results demonstrate that the interactions between protein polymer and t-CNC are not exclusively dictated by charge neutralization. The E homopolymer interacts with t-CNCs, as demonstrated by the slight blue shift and increase in structure via CD, while the C homopolymer rigid, coil structure remains unaltered (Figure 5). Thus E, which is presumably neutral in charge and more flexible, binds and interacts with t-CNC (Figure 6). This suggests that the mode of t-CNC and protein polymer interaction is predominantly hydrophobic especially in light of cellulose bearing a hydrophobic face. While cellulose nanocrystals possess a hydrophilic edge, they possess a hydrophobic side in its ribbon like structure.[66] The appropriate combination of hydrophobic side chains with flexible conformation from E and positive charge demonstrated by CE provides the best interface with t-CNCs, leading to the most significant changes in viscoelastic properties (Figures 2 and 7). By contrast, EC bears significantly more positive surface charge and rigid helical structure, leading to weaker interactions with t-CNC and lack of synergistic changes in viscoelastic property (Figures 6 and 7).

Interplay between structure and self-assembly of the protein block polymers. A relationship between the folding and overall assembly of the EC and CE protein polymers is evident from these studies. While EC and CE are compositionally similar, the orientation of the E and C domain impacts the secondary structure and self-assembly as has been revealed in previous studies.[17−20] The wavelength scans of EC and CE differ (Figure 5), and this result is a discrepancy in the particle assembly as confirmed by zeta potential analysis. The difference in the protein diblock conformation influences the ability to further self-assemble into particles, resulting in the observed particle surface charge difference. While the EC polymer exhibits a positive surface charge, predominantly characteristic of the C domain, CE is less positive in magnitude, indicative of the fact that the surface displays E-like character (Figures 6 and 7). This discrepancy in surface charge confirms that block orientation impacts the packing and overall self-assembly leading to the subsequent interactions with t-CNC as described below.

Effects of t-CNCs Across Different Length Scales, Leading to Enhanced Viscoelastic Properties. Our results demonstrate that t-CNCs affects the protein polymers on the nanoscale. The strength of t-CNC interactions with the protein polymers is dependent on the folding and assembly of the protein polymers, leading to different surface characteristics. All the methodologies employed to characterize the interactions between the EC and CE with t-CNCs confirm that there is a strong interaction between the t-CNCs with the E domain within the protein polymers (Figure 7). On the nanoscale level, protein conformational analysis via CD shows the E domain of the two block polymers responsible for the interactions with t-

dx.doi.org/10.1021/bm401304w | *Biomacromolecules* 2013, 14, 4360−4367

CNC (Figure 5). On the microscale level, the surface charge of the supramolecular particles differs between EC and CE in which CE exhibits a predominantly E-like surface in contrast to the EC (Figure 6). This difference in surface of EC and CE protein polymers influences the interactions with the t-CNCs and impacts the overall mechanical properties of the bionanocomposite as demonstrated (Figure 1, and Figure 6). Moreover, confocal microscopy data reveal that the mixture of CE+t-CNC possessed more interspersed particles and smaller domains of t-CNCs relative EC+t-CNC (Figure 4). This led to the formation of elastic networks in case of the CE+t-CNC mixture with more random entanglement when compared to EC+t-CNC.

Insight from Nature: Cellulose Binding Domains. Cellulose binding domains (CBDs)[32] in natural proteins can provide insight into protein and cellulose interactions. Three salient features of CBDs are: (1) conformation, (2) surface characteristics and (3) interactions with cellulose. CBDs are predominantly comprised of β-structures. For example, C_{ex}CBD, a member of category 2 from β-1,4-glycanase of *Cellulomonas fimi*, exhibits a nine-stranded β-barrel with three solvent-exposed tryptophans and hydrophilic residues for cellulose binding.[67] CBD_{NI} in category 4, from CenC cellulase *Cellulomonas fimi*, is composed of 10 β-strands folded into two antiparallel β-sheets.[68] CBD_{Cip} from the cellulosomal subunit *Clostridium thermocelum* in category 3, possesses a 9 stranded β-sandwich with a line of polar/aromatic residues to interact with cellulose.[35] Category 5 member CBD_{EGZ}, from *Erwinia chrysanthemi,* exhibits a triple antiparallel β-sheet orthogonal to a loop as well as three residues with aromatic rings for cellulose binding.[69] More importantly, this protein has a hydrophobic surface that is easily accessible and the surface area of the structure is comprised of 69% of nonpolar residues.[69−71] Similarly, category 1 CBD_{CBHI}, from *Trichoderma reesei*, possesses an irregular β-sheet with a hydrophobic surface comprised of three tyrosine residues for cellulose binding.[72−74] Although these proteins display slight differences in their β-like conformations, they all share a concave groove near their surfaces for cellulose binding. Notably, some of the binding sites are equipped with two or more aromatic side chains, which can interact with cellulose via van der Waals interactions.[67,75−79] In addition, CBDs tend to aggregate in aqueous solutions because of their hydrophobic character.[67,80] Our experimental evidence of t-CNCs interacting with the exposed β-like E domain via hydrophobic interactions is consistent with these observations.

CONCLUSIONS

Surprisingly, CE+t-CNC displays a dynamic change in viscoelastic properties as a function of time, leading to elastic networks when compared to the EC+t-CNC. Moreover, the difference in structure and assembly of the protein block polymers influences its overall interactions with t-CNCs. The extent of interaction with t-CNC appears to be dictated by the surface character of the protein block polymer when assembled into particles. Since CE exhibits a more E dominated surface, it exhibits a stronger interaction with a concomitant elastic network with t-CNCs. Our results affirm that protein folding and assembly is critical to understanding how a protein polymer can interact with other biopolymers including t-CNCs especially upon curing as a function of time. Lessons learned from these experiments may provide insights into the design of future bionanocomposites.

ASSOCIATED CONTENT

Supporting Information

SDS-page of proteins, conjugation procedure of Alexa Fluor 555 succinimidyl ester to block polymers, conjugation procedure of FITC to t-CNC nanowhiskers, CD spectra of t-CNC, MSD plots of proteins and t-CNC alone after 10 and 100 min, and time cure superposition plot showing the "pre-gel" and "post-gel" plots for CE+t-CNC. This material is available free of charge via the Internet at http://pubs.acs.org."

AUTHOR INFORMATION

Corresponding Author

*E-mail: jmontcla@poly.edu.

Notes

A portion of this work was carried out by the National Institute of Standards and Technology (NIST), an agency of the U.S. government, and by statute is not subject to copyright in the United States. Certain commercial equipment, instruments, materials, services, or companies are identified in this paper in order to adequately specify the experimental procedure. This in no way implies endorsement or recommendation by NIST.
The authors declare no competing financial interest.

ACKNOWLEDGMENTS

This work was supported by the AFOSR FA-9550-07-1-0060, and FA-9550-08-1-0266 (J.K.M.), NSF DMR-1205384 (J.K.M.), NSF DMR-1006407 (R.S.T.), AFOSR-MIPR FIA-TA02045G002 (J.W.G. and I. S.) in part by the NSF MRSEC Program under Award Number DMR-0820341, Society of Plastic Engineers (J.S.H.), GK-12 Fellows Grant DGE-0741714 (J.S.H.), Swiss National Science Foundation (National Research Programme 64, Project #406440_131264/1)(S.M.) and the Adolphe Merkle Foundation (S.M., C.W., E.J.F.).

REFERENCES

(1) Dickerson, M. B.; Sandhage, K. H.; Naik, R. R. *Chem. Rev.* **2008**, *108*, 4935.
(2) Aizenberg, J.; Tkachenko, A.; Weiner, S.; Addadi, L.; Hendler, G. *Nature* **2001**, *412*, 819.
(3) Brott, L. L.; Naik, R. R.; Pikas, D. J.; Kirkpatrick, S. M.; Tomlin, D. W.; Whitlock, P. W.; Clarson, S. J.; Stone, M. O. *Nature* **2001**, *413*, 291.
(4) Aizenberg, J.; Hendler, G. *J. Mater. Chem.* **2004**, *14*, 2066.
(5) Kramer, R. M.; Crookes-Goodson, W. J.; Naik, R. R. *Nat. Mater.* **2007**, *6*, 533.
(6) Izumi, M.; Sweeney, A. M.; Demartini, D.; Weaver, J. C.; Powers, M. L.; Tao, A.; Silvas, T. V.; Kramer, R. M.; Crookes-Goodson, W. J.; Mäthger, L. M.; Naik, R. R.; Hanlon, R. T.; Morse, D. E. *J. R. Soc. Interface* **2010**, *7*, 549.
(7) Tao, A. R.; DeMartini, D. G.; Izumi, M.; Sweeney, A., M.; Holt, A. L.; Morse, D. E. *Biomaterials* **2010**, *31*, 793.
(8) Martens, A. A.; Gucht, J. V. D.; Eggink, G.; Wolf, F. A. D.; Stuart, M. A. C. *Soft Matter.* **2009**, *5*, 4191.
(9) Dandu, R.; Megeed, Z.; Haider, M.; Cappello, J.; Ghandehari, H. *ACS Symposium* **2006**, *924*, 150.
(10) Creighton, T. E. 2nd ed. ed.; W.H. Freeman and Company: New York, 1997.
(11) Teramoto, A.; Takagi, Y.; Hachimori, A.; Abe, K. *Polym. Adv. Technol.* **1999**, *10*, 681.
(12) De Kruif, C. G.; Weinbreck, F.; de Vries, R. *Curr. Opin. Colloid Interface Sci.* **2004**, *9*, 340.
(13) Doublier, J. L.; Garnier, C.; Renard, D.; Sanchez, C. *Curr. Opin. Colloid Interface Sci.* **2000**, *5*, 202.
(14) Larionova, N. I.; Unksova, L. Y.; Mironov, V. A.; Sakharov, I. Y.; Kazanskaya, N. F.; Berezin, I. V. *Polym. Sci. U.S.S.R.* **1981**, *23*, 1999.

(15) Chung, W.-J.; Kwon, K.-Y.; Song, J.; Lee, S.-W. *Langmuir* **2011**, *27*, 7620.
(16) Wang, E.; Lee, S.-H.; Lee, S.-W. *Biomacromolecules* **2011**, *12*, 672.
(17) Haghpanah, J. S.; Yuvienco, C.; Civay, D. E.; Barra, H.; Baker, P. J.; Khapli, S.; Voloshchuk, N.; Gunasekar, S. K.; Muthukumar, M.; Montclare, J. K. *ChemBioChem* **2009**, *10*, 2733.
(18) Haghpanah, J. S.; Yuvienco, C.; Roth, E. W.; Liang, A.; Tu, R. S.; Montclare, J. K. *Mol. BioSyst.* **2010**, *6*, 1662.
(19) Dai, M.; Haghpanah, J.; Singh, N.; Roth, E. W.; Liang, A.; Tu, R. S.; Montclare, J. K. *Biomacromolecules* **2011**, *12*, 4240.
(20) Yuvienco, C.; More, H. T.; Haghpanah, J. S.; Tu, R. S.; Montclare, J. K. *Biomacromolecules* **2012**, *13*, 2273.
(21) Samir, M. A. S. A.; Alloin, F.; Dufresne, A. *Biomacromolecules* **2005**, *6*, 612.
(22) Eichhorn, S. J. *Soft Matter* **2011**, *7*, 303.
(23) Lima, M. M. D. S.; Wong, J. T.; Paillet, M.; Borsali, R.; Pecora, R. *Langmuir* **2003**, *19*, 24.
(24) Favier, V.; Chanzy, H.; Cavaille, J. Y. *Macromolecules* **1995**, *28*, 6365.
(25) Dufresne, A.; Kellerhals, M. B.; Witholt, B. *Macromolecules* **1999**, *32*, 7396.
(26) Šturcová, A.; Davies, G. R.; Eichhorn, S. J. *Biomacromolecules* **2005**, *6*, 1055.
(27) Jorfi, M.; Roberts, M. N.; Foster, E. J.; Weder, C. *ACS Appl. Mater. Interfaces* **2013**, *5*, 1517.
(28) Ruiz, M. M.; Cavaille, J. Y.; Dufresne, A.; Graillat, C.; J-F., G. *Macromol. Symp.* **2001**, *169*, 221.
(29) Capadona, J. R.; Shanmuganathan, K.; Tyler, D. J.; Rowan, S. J.; Weder, C. *Science* **2008**, *319*, 1370.
(30) Capadona, J. R.; Van Den Berg, O.; Capadona, L. A.; Schroeter, M.; Rowan, S. J.; Tyler, D. J.; Weder, C. *Nat. Nanotechnol.* **2007**, *2*, 3.
(31) Shanmuganathan, K.; Capadona, J. R.; Rowan, S. J.; Weder, C. *Prog. Polym. Sci.* **2010**, *35*, 212.
(32) Mathew, A. P.; Dufresne, A. *Biomacromolecules* **2002**, *3*, 609.
(33) Whittle, D. J.; Kilburn, D. G.; Warren, R. A. J.; Miller, R. C., Jr *Gene* **1982**, *17*, 139.
(34) Tomme, P.; Warren, R. A. J.; Gilkes, N. R. Cellulose Hydrolysis by Bacteria and Fungi. In *Advances in Microbial Physiology*; Poole, R. K., Ed.; Academic Press: London, U.K., 1995.
(35) Gilkes, N. R.; Henrissat, B.; Kilburn, D. G.; Miller, R. C.; Warren, R. A. *Am. Soc. Microbiol.* **1991**, *55*, 303.
(36) Tormo, J.; Lamed, R.; Chirino, A. J.; Morag, E.; Bayer, E. A.; Shoham, Y.; Steitz, T. A. *EMBO J.* **1996**, *15*, 5739.
(37) Xu, G.-Y.; Ong, E.; Gilkes, N. R.; Kilburn, D. G.; Muhandiram, D. R.; Harris-Brandts, M.; Carver, J. P.; Kay, L. E.; Harvey, T. S. *Biochemistry* **1995**, *34*, 6993.
(38) Johnson, P. E.; Joshi, M. D.; Tomme, P.; Kilburn, D. G.; McIntosh, L. P. *Biochemistry* **1996**, *35*, 14381.
(39) Brun, E.; Moriaud, F.; Gans, P.; Blackledge, M. J.; Barras, F.; Marion, D. *Biochemistry* **1997**, *36*, 16074.
(40) Richards, F. M. *J. Mol. Biol.* **1974**, *82*, 1.
(41) Richmond, T. J. *J. Mol. Biol.* **1984**, *178*, 63.
(42) Reinikainen, T.; Teleman, O.; Teeri, T. T. *Proteins* **1995**, *22*, 392.
(43) Linder, M.; Mattinen, M. L.; Kontteli, M.; Lindeberg, G.; Ståhlberg, J.; Drakenberg, T.; Reinikainen, T.; Pettersson, G.; Annila, A. *Protein Sci.* **1995**, *4*, 1056.
(44) Kraulis, P. J.; Clore, G. M.; Nilges, M.; Jones, T. A.; Pettersson, G.; Knowles, J.; Gronenborn, A. M. *Biochemistry* **1989**, *28*, 7241.
(45) Poole, D. M.; Hazlewood, G. P.; Huskisson, N. S.; Virden, R.; Gilbert, H. J. *FEMS Microbiol. Lett.* **1993**, *106*, 77.
(46) Nagy, T.; Simpson, P.; Williamson, M. P.; Hazlewood, G. P.; Gilbert, H. J.; Orosz, L. *FEBS Lett.* **1998**, *429*, 312.
(47) Gusakov, A. V.; Sinitsyn, A. P.; Berlin, A. G.; Markov, A. V.; Ankudimova, N. V. *Enzyme Microb. Technol.* **2000**, *27*, 664.
(48) Linder, M.; Nevanen, T.; Teeri, T. T. *FEBS Lett.* **1999**, *447*, 13.
(49) Srisodsuk, M.; Lehtiö, J.; Linder, M.; Margolles-clark, E.; Reinikainen, T.; Teeri, T. T. *J. Biotechnol.* **1997**, *57*, 49.
(50) levy, I.; Nussinovitch, A.; Shpigel, E.; Shoseyov, O. *Cellulose* **2002**, *9*, 91.
(51) van den Berg, O.; Capadona, J. R.; Weder, C. *Biomacromolecules* **2007**, *8*, 1353.
(52) Corrigan, A.; Donald, A. *Eur. Phys. J. E: Soft Matter Biol. Phys.* **2009**, *28*, 457.
(53) Corrigan, A. M.; Donald, A. M. *Soft Matter* **2010**, *6*, 4105.
(54) Crocker, J. C.; Grier, D. G. *J. Colloid Interface Sci.* **1996**, *179*, 298.
(55) Yao, A.; Tassieri, M.; Padgett, M.; Cooper, J. *Lab Chip* **2009**, *9*, 2568.
(56) Breedveld, V.; Pine, D. J. *J. Mater. Sci.* **2003**, *38*, 4461.
(57) Mason, T. G.; Ganesan, K.; van Zanten, J. H.; Wirtz, D.; Kuo, S. C. *Phys. Rev. Lett.* **1997**, *79*, 3282.
(58) Mason, T. G.; Weitz, D. A. *Phys. Rev. Lett.* **1995**, *74*, 1250.
(59) Schneider, J. P.; Pochan, D. J.; Ozbas, B.; Rajagopal, K.; Pakstis, L.; Kretsinger, J. *J. Am. Chem. Soc.* **2002**, *124*, 15030.
(60) Veerman, C.; Rajagopal, K.; Palla, C. S.; Pochan, D. J.; Schneider, J. P.; Furst, E. M. *Macromolecules* **2006**, *39*, 6608.
(61) Winter, H. H.; Chambon, F. *J. Rheol.* **1986**, *30*, 367.
(62) Hess, W.; Vilgis, T. A.; Winter, H. H. *Macromolecules* **1988**, *21*, 2536.
(63) Larsen, T.; Schultz, K.; Furst, E. M. *Korea-Aust. Rheol. J.* **2008**, *20*, 165.
(64) Adolf, D.; Martin, J. E. *Macromolecules* **1990**, *23*, 3700.
(65) Stauffer, D.; Coniglio, A.; Adam, M. Gelation and critical phenomena. In *Polymer Networks*, Dušek, K., Ed.; Springer: Berlin, 1982.
(66) Glasser, W.; Atalla, R.; Blackwell, J.; Malcolm Brown, R., Jr.; Burchard, W.; French, A.; Klemm, D.; Nishiyama, Y. *Cellulose* **2012**, *19*, 589.
(67) Joanny, J. F. *J. Phys. (Paris)* **1982**, *43*, 467.
(68) Larsen, T. H.; Branco, M. C.; Rajagopal, K.; Schneider, J. P.; Furst, E. M. *Macromolecules* **2009**, *42*, 8443.
(69) Savitzky, A.; Golay, M. J. E. *Anal. Chem.* **1964**, *36*, 1627.
(70) Muthukumar, M. *Macromolecules* **1989**, *22*, 4656.
(71) Scanlan, J. C.; Winter, H. H. *Macromolecules* **1991**, *24*, 47.
(72) Nystroem, B.; Walderhaug, H.; Hansen, F. K.; Lindman, B. *Langmuir* **1995**, *11*, 750.
(73) Antonietti, M.; Foelsch, K. J.; Sillescu, H.; Pakula, T. *Macromolecules* **1989**, *22*, 2812.
(74) Richtering, H. W.; Gagnon, K. D.; Lenz, R. W.; Fuller, R. C.; Winter, H. H. *Macromolecules* **1992**, *25*, 2429.
(75) Lin, Y. G.; Mallin, D. T.; Chien, J. C. W.; Winter, H. H. *Macromolecules* **1991**, *24*, 850.
(76) Raghavan, S. R.; Douglas, J. F. *Soft Matter* **2012**, *8*, 8539.
(77) Martin, S. R.; Schilstra, M. J. *Methods Cell Biol.* **2008**, *84*, 264.
(78) Gunasekar, S. K.; Asnani, M.; Limbad, C.; Haghpanah, J. S.; Hom, W.; Barra, H.; Nanda, S.; Lu, M.; Montclare, J. K. *Biochemistry* **2009**, *48*, 8559.
(79) Gunasekar, S. K.; Anjia, L.; Matsui, H.; Montclare, J. K. *Adv. Funct. Mater.* **2012**, *22*, 2154.
(80) Rusli, R.; Shanmuganathan, K.; Rowan, S. J.; Weder, C.; Eichhorn, S. J. *Biomacromolecules* **2011**, *12*, 1363.